## **Inorganic Chemistry**

pubs.acs.org/IC Article

# Thiolate-Thione Redox-Active Ligand with a Six-Membered Chelate Ring via Template Condensation and Its Pt(II) Complexes

Linda A. Zuckerman, Natasha P. Vargo, Claire V. May, Michael P. Crockett, Ariel S. Hyre, James McNeely, Jessica K. Elinburg, Alexander M. Brown, Jerome R. Robinson, Arnold L. Rheingold, and Linda H. Doerrer\*



Cite This: Inorg. Chem. 2021, 60, 13376-13387



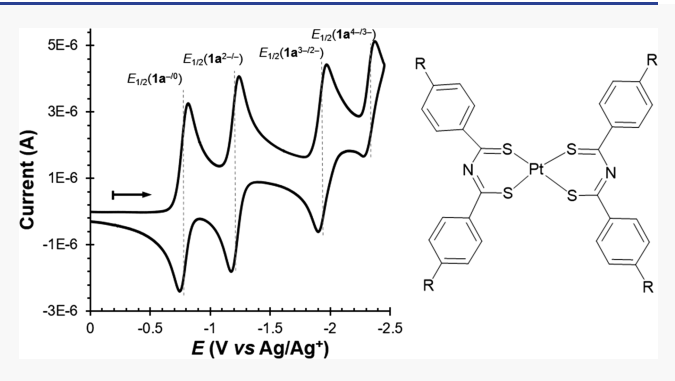
ACCESS

III Metrics & More

Article Recommendations

sı Supporting Information

**ABSTRACT:** A new template condensation reaction has been discovered in a mixture of Pt(II), thiobenzamide, and base. Four complexes of the general form  $[Pt(ctaPh^R)_2]$ ,  $R = CH_3$  (1a), H (1b), F (1c), Cl (1d), Cl (1e), Cl (1d), Cl (1e), Cl (1d), Cl (1e), Cl (1d), Cl (1e), Cl (1e



magnetization. The singly reduced form containing  $[1a]^{1-}$ ,  $(nBu_4N)[Pt(ctaPh^{CH3})_2]$ , has been generated in situ and characterized by UV–vis and EPR spectroscopies. DFT studies of 1b,  $[1b]^{1-}$ , and  $[1b]^{2-}$  confirm the location of additional electrons in exclusively ligand-based orbitals. A detailed analysis of this redox-active ligand, with emphasis on the characteristics that favor noninnocent behavior in six-membered chelate rings, is included.

#### INTRODUCTION

Chelating redox-active ligands were first investigated intensely in the 1960s when the redox activity of dithiolene ligands was demonstrated and explained. <sup>1,2</sup> Isoelectronic catecholate <sup>3</sup> and closely related benzene dimine <sup>4</sup> and aminophenolate <sup>5,6</sup> ligands were also studied extensively. A second profusion of research in redox-active ligands occurred after 2000, when the redox chemistry of 2,6-diiminopyridine ligands, recognized by Weighardt, <sup>7</sup> came to be widely appreciated. <sup>8</sup> All three of these large groups of redox-active ligands have five-membered chelate rings. The use of noninnocent ligands in many areas of research continues to grow, and numerous reviews are available. <sup>9–19</sup>

Ligands that form six-membered chelate rings can also be redox active, although they are less numerous than five-membered ones. A concise overview of noninnocent ligands with three-, four-, six-, and seven-membered rings has recently appeared.<sup>20</sup> Shown in Scheme 1 is a survey of redox-active ligands with six-membered chelate rings, to give an overview of the chemical diversity in this area, which is not comprehensive or chronological. As with five-membered chelate rings, a variety of *p*-block elements as donor atoms are known. With O-donors, (a) [Cr(hfac)<sub>2</sub>(pyz)<sub>2</sub>] contains Cr(III), a dianionic radical hexafluoroacetylacetonate (hfac) and pyrazine ligands<sup>21,22</sup> whereas (b) has two 9-oxidophenalenone ligands<sup>23</sup>

which, analogous to quinones, can exist in three different redox states. <sup>24,25</sup> Salen- and salan-type ligands, example (c), <sup>26</sup> can be redox active through the iminophenolate moiety. In the center row, (d) is S = 1 [Ni(NacNac)<sub>2</sub>] whose singly oxidized form, [Ni(NacNac)<sub>2</sub>]<sup>+</sup>, shows loss of a fractional 0.80 spin from the ligand and only 0.20 from the metal center. 27 A Zn analog can be electrochemically oxidized by two electrons, and calculations for that product suggest a triplet state.<sup>27</sup> One reduced Fe complex contains a redox innocent NacNac and two nitrile ligands.<sup>28</sup> In general, such  $\beta$ -diketiminate ligands can be redox noninnocent if there are reducible groups in the 2- and 4positions<sup>29</sup> whose orbitals extend the  $\pi$  system and lower its energy. The dipyrrin moiety, shown in (e),30 like the larger porphyrins, is redox active,<sup>31</sup> as are the pyrrole rings in the nindigo ligand in (f). 32,33 Example (g) shows the more N-rich dihydrazonopyrrole ligand,<sup>34</sup> (h) has the bi(imidazolylketone) ligand, 35 and two formazanate ligands are found in the homoleptic Zn complex in (i).36 The unusual compound (j)

Received: June 3, 2021 Published: August 12, 2021





Scheme 1. Examples of Redox-Active Ligands That Form Six-Membered Chelate Rings, with References in the Main Text<sup>a</sup>

$$(a) \qquad (b) \qquad (c) \qquad (c) \qquad (c) \qquad (d) \qquad (e) \qquad (f) \qquad (g) \qquad (g)$$

"(a) hfac, (b) 9-oxidophenalenone, (c) salan, (d) nacnac, (e) dipyrrin, (f) nindigo, (g) dihydrazonopyrrole, (h) bi(imidazolylketone), (i) formazanate, (j) bis(diphenylphosphino)naphthalene, (k), SacSac. The p-block elements that form the chelate ring are highlighted in blue.

with a redox-active P-donor ligand is a precatalyst for  $H^+$  reduction, whose DFT studies support significant radical character for the reduced form of the dppn (bis-(diphenylphosphino)naphthalene) ligand. Early work with S^S donor systems included complexes of SacSac ligands, example (k), which exhibited redox activity, but have scarcely been developed to date, perhaps for reasons to be discussed below.  $^{39-41}$ 

Herein, we report a serendipitous discovery of a new, redoxactive six-membered chelate ring with two S-donor atoms. In recent years, numerous heterobimetallic lantern (paddlewheel) complexes with thiocarboxylate ligands were prepared. 42-48 These compounds are of interest as building blocks for quasi-1D structures including dimers and extended chains with unusual magnetic<sup>49–51</sup> properties. Thiocarboxylate ligands have ensured clean preparation in good yields of these complexes because the soft S donor binds well to soft metals such as Pt and Pd, 42,51 while the harder O donor binds to a variety of 3d and s block metals. To develop a greater variety of building blocks, we decided to change the hard donor from O to NH. Bimetallic lantern complexes with S^N donor ligands are known with monothiosuccinimide, 52-54 thioxopiperidinone,<sup>54</sup> mercaptopyridine,<sup>55–58</sup> and thiocaprolactam<sup>56,59</sup> but not with thioamides that we are aware.

When previously successful synthetic methods were applied to S^N donor thiobenzamide, no lantern complexes resulted, but rather a new Pt-containing compound with new S^S donor ligands formed by template condensation was obtained. Control experiments without the 3d metal indicated that it is not required to form the new Pt(II) compound. This family of compounds is important because it contains an entirely new

group of redox-active ligands, condensed thioamides (cta), formed by template condensation, and because the redox-active ligands form six-membered chelate rings. Herein, we report the detailed experimental and computational studies of  $[Pt(ctaPh^R)_2]$  ( $R = CH_3$ , H, F, and Cl), which provide the first structural characterization of a reduced S^S donor six-membered chelate ring, and put these results in the context of other redox-active ligands.

## RESULTS

An analogous synthesis to the thiocarboxylate lantern complexes was attempted with thiobenzamide, in which 1 equiv each of Pt and a 3d transition metal were added to 4 equiv each of PhC(S)NH and NaHCO3. A deep green color developed rapidly, and a precipitate formed, which was recrystallized and shown by single-crystal X-ray diffraction to be a mononuclear Pt(II) compound with {S<sub>4</sub>} coordination from two new bidentate ligands forming six-membered chelate rings, as shown in Scheme 2. This condensation occurs reproducibly for four para-substituted starting thiobenzamides (R = CH<sub>3</sub> (1a), H (1b), F (1c), Cl (1d)), but only intractable mixtures were obtained with alkyl substituted thioamides including thioacetamide ((H2NC(S)CH3)3) and 2-phenylthioacetamide (H2NC(S)CH2Ph). Some stabilization of the central imine N may occur through intramolecular C-H···N hydrogen-bonding interactions with the ortho H atoms of the slightly rotated phenyl rings (see structural discussion below).

Based on its composition, we have named this new family of ligands condensed thioamides, (ctaPh<sup>R</sup>), with a Ph substituent on the sp<sup>2</sup> carbon and a *para* substituent R on these phenyl rings. The proposed mechanism of {cta}<sup>-</sup> formation is shown

Scheme 2. Synthesis and Unexpected Structure of 1a-1d

4 
$$+$$
 4 KHCO<sub>3</sub>  $\xrightarrow{K_2PtCl_4}$   $+$  8  $\times$  8  $\times$  8  $\times$  9  $\times$  1  $\times$ 

in Scheme 3. Initial binding of thiobenzamide, deprotonated or not, to Pt is reasonable. One deprotonated thiobenzamide can attack the thiocarbonyl carbon atom of an adjacent thiobenzamide to form a new C-N bond. Subsequent loss of NH3 leads to the six-membered chelate ring and a monoanionic, bidentate ligand. Complex 1a was found to undergo a two-electron reduction with the addition of Cp2Co in THF to yield  $[Cp_2Co]_2[1a]$ ,  $[Cp_2Co]_2[Pt(ctaPh^{CH3})_2]$ . Both reagents and products are highly soluble in THF, but careful concentration of the filtrate under reduced pressure and cooling for several hours at -30 °C results in the selective crystallization of [Cp<sub>2</sub>Co]<sub>2</sub>[1a], as dark purple crystalline plates in 70-80% crystalline yield. Repeated attempts to prepare and isolate a salt containing the monoanion [Pt- $(ctaPh)_2]^{1-}$ ,  $[1a]^{1-}$ , in Scheme 4, were unsuccessful. The dianion and neutral form do not comproportionate, from which mixture only the neutral form is successfully isolated. Both stoichiometric reduction from [Pt(ctaPh<sup>CH3</sup>)<sub>2</sub>] with 1 equiv of  $[Cp_2Co]$  or  $[Cp^*_2Fe]$  and one-electron oxidation attempts of  $[Pt(ctaPh^{CH3})_2]^{2-}$  with  $Ag^+$  or  $[Cp_2Fe]^+$  were unsuccessful. Other experimental data (spectroelectrochemistry, EPR spectroscopy), however, indicate stability of this radical form in situ, as discussed below.

## **■ STRUCTURAL CHARACTERIZATION**

The parent compound 1a is 2-fold symmetric with an inversion center at the square-planar Pt atom. As shown on the left-hand side of Figure 1, the four Pt–S distances (Table S1) are nearly equivalent and average 2.2843(7) Å and are slightly shorter than the average Pt–S distance of 2.40(3) Å from ~450 structurally characterized {PtS<sub>4</sub>} centers. The chelating S–Pt–S angle subtended by the cta ligand is 97.40(2)°, while the open S–Pt–S angle between two different ligands is 82.60(2)°. The Pt atom is displaced only 0.007 Å from the best {S<sub>4</sub>} plane with a  $\tau_4$  value of 0, while the torsion angle between the best {PtS<sub>2</sub>} plane and its respective chelate {S<sub>2</sub>C<sub>2</sub>} is only 4.40°. Altogether, these parameters indicate a typical planar four-coordinate environment at Pt.

The metrical parameters within the ligand of **1a** are also broadly consistent with the Lewis structures shown in Schemes 2, 3 and 5, where there is significant partial multiple bond

character delocalized in the chelate ring. Although the ligand is drawn with an asymmetric thione-thiolate structure in Scheme 2, all data to date suggest that the ligands are 2-fold symmetric about their central N atom with all five p-block atoms in the chelate ring being  $sp^2$  hybridized. Compound 1a displays four virtually identical S–C (average: 1.705(2) Å) and C–N (1.324(3) Å) bonds, which are clearly intermediate between that of typical S–C and C–N single (1.82 and 1.47 Å) and double bonds (1.60 and 1.28 Å).

Single-crystal X-ray diffraction (SCXRD) data for compound 1b were of sufficient quality to determine only the connectivity (Figure S2). SCXRD data for compounds 1c and 1d, shown in Figures S3 and S4, respectively, allow comparison to the parent compound 1a, and the core metrical parameters are given in Table S1. There are no substantial differences in the molecular cores relating to either the Pt coordination by S or the structures of the chelate rings. As in 1a, the Pt center and two chelate rings in 1c and 1d form a delocalized  $\pi$  system. The average torsion angles (deg) between the phenyl rings and the chelate rings are sufficient such that the phenyl groups are not strongly conjugated with the chelate rings but are rotated out of the {PtS<sub>4</sub>} plane by 19.0 (1a), 32.8 (1c), and 26.7 (1d). These rotations hinder intermolecular  $\pi - \pi$  stacking and increase the Pt···Pt distances. The shortest intermolecular Pt···Pt contact in 1a is 8.9 Å, too long for a potential metallophilic interaction (generally accepted as possible at less than the sum of two van der Waals radii, 3.44 Å for Pt).<sup>63</sup> The shortest Pt···Pt contacts in 1c and 1d are 3.849 and 3.802 Å, respectively, which are less than half the Pt-Pt distance in 1a, but still not metallophilic.

The doubly reduced compound [Cp2Co]2[1a] has slightly longer Pt-S bonds than its neutral counterpart, with an average of 2.295(2) Å, consistent with a constant Pt(II) oxidation state and two additional electrons being located in the chelate ring  $\pi$ -systems and increased occupation of a Pt-S antibonding orbital. The biggest difference between the neutral and doubly reduced compounds is the significant bend between the {PtS<sub>4</sub>} core and the chelate ring in the latter. This feature is discussed in more detail below (see Scheme 6) in the context of the magnetic properties. The S-C and C-N bonds also increased on average to 1.753(9) Å and 1.33(1) Å, respectively. A graphical comparison of the differences in the intraligand distances for 1a and [Cp2Co]2[1a] is given in Figure S6. The intraligand S-Pt-S angles decrease from  $97.40(2)^{\circ}$  in the neutral parent to an average of  $94.52(7)^{\circ}$ , while the interligand angles increase to 85.48(7)° from 82.60(2)°.

## ■ NMR AND UV-VIS SPECTROSCOPIES

The <sup>1</sup>H NMR spectra for all four compounds show the expected resonances for the phenyl ring and are consistent with free rotation of the phenyl rings about the C–C bonds. The RT electronic absorption spectra of **1a–1d** are overlaid in Figure S7 and show absorbances at the expected energies,

Scheme 3. Proposed Mechanism of Formation of a Single (cta<sup>Ph</sup>) Ligand

Scheme 4. Chemical and Electrochemical Reduction Reactions of 1

Figure 1. ORTEPs of 1a (left) and the anion of  $[Cp_2Co]_2[1a]$  (right). Ellipsoids at 50% level. Hydrogen atoms and  $[Cp_2Co]^+$  cations removed for clarity.

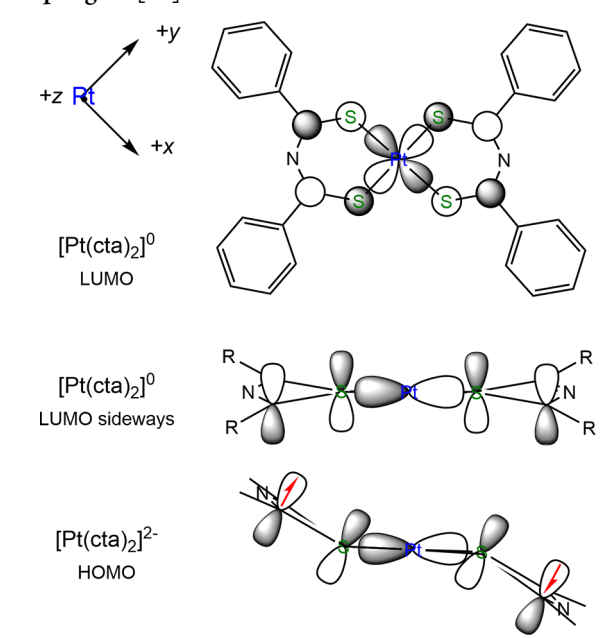
Scheme 5. Three Redox States of the {cta<sup>R</sup>} Ligand

including intense ILCT features between 230–450 nm and strong MLCT/LMCT  $\sim 600$  nm.  $^{64}$  Because a MLCT process is a transient version of a chemically induced reduction of the ligand, the strong MLCT suggests that the ligand could be chemically reduced by one or more electrons, to form correspondingly one or more new compounds. Such behavior was conclusively demonstrated in the synthesis of  $[\text{Cp}_2\text{Co}]_2[1a]$  and with further spectroelectrochemical characterization below. The RT  $^1\text{H}$  NMR data for  $[\text{Cp}_2\text{Co}]_2[1a]$  indicate paramagnetism, which property is described in detail next.

## **■ MAGNETISM**

The magnetic susceptibility of  $[Cp_2Co]_2[Pt(ctaPh^{CH3})_2]$ ,  $[Cp_2Co]_2[1a]$ , was measured at a constant field of 5000 Oe over the temperature range of 4 to 300 K (Figure 2). The  $\chi T$ 

Scheme 6. Orbital Overlaps in Generic 1 (Top and Middle, LUMO) and  $[1]^{2-}$  (Bottom, HOMO) That Explain AF Coupling in  $[1a]^{2-}$ 



versus T data, after diamagnetic corrections with Pascal's constants, are shown in green, along with the fit (black) determined with PHI.<sup>65</sup> Field-dependent magnetization

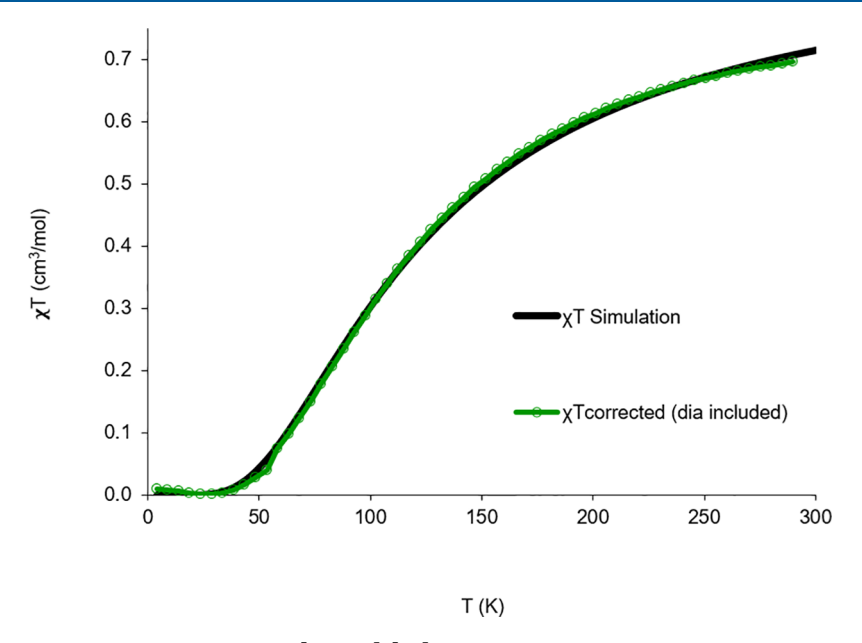


Figure 2. Variable-temperature magnetic susceptibility of  $[Cp_2Co]_2[1a]$  at 5000 Oe.

Table 1. E<sub>1/2</sub> Values Obtained from Cyclic Voltammetry Experiments of 1a-1c (2.5 mM) Performed in THF<sup>a</sup>

| complex   | $E_{1/2}(1^{-/0})^{b}$ | $E_{1/2}(1^{2-/-})^{b}$ | $E_{1/2}(1^{3-/2-})^{b}$ | $E_{1/2}(1^{4-/3-})^{b}$ |
|---|------------------------|-------------------------|--------------------------|--------------------------|
| $[Pt(ctaPh^{CH3})_2] (1a)$  | -0.77                  | -1.18                   | -1.93                    | -2.29                    |
| $[Pt(ctaPh^{H})_{2}] (1b)$  | -0.74                  | - 1.13                  | -1.87                    | -2.26                    |
| $[Pt(ctaPh^F)_2]$ (1c)  | -0.66                  | -1.10                   | -1.91                    | -2.40                    |
| <sup>a</sup> Measured using a 3 mm glassy carbon electrode; $\nu = 100$ mV/s; $[NBu_4][PF_6] = 250$ mM $E_{1/2} = (E_{p,a} + E_{p,c})/2$ . <sup>b</sup> Volts vs Ag/Ag <sup>+</sup> . |                        |                         |                          |                          |

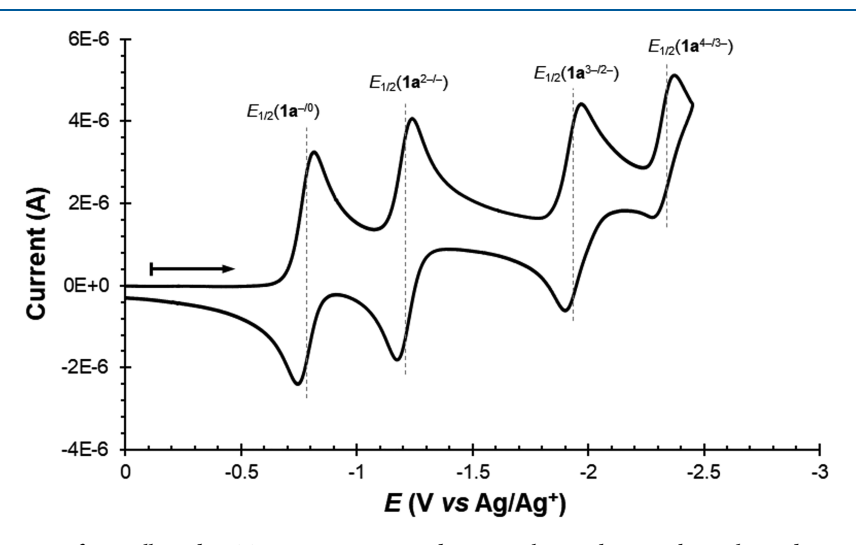


Figure 3. Cyclic voltammogram of 1a collected in THF using a 3 mm diameter glass carbon working electrode;  $\nu = 10$  mV/s; [1a] = 1 mM;  $[NBu_4][PF_6] = 200$  mM.

measurements performed on microcrystalline  $[\mathbf{Cp_2Co}]_2[\mathbf{1a}]$  at 100 K confirmed the absence of ferromagnetic impurities (Figure S8). The  $\chi T$  value is effectively zero below 50 K but steadily increases to  $\sim 0.7$  cm<sup>3</sup>/mol at 300 K. This curve is indicative of a low-lying triplet state above a singlet ground state that is dominant at lower temperatures, confirming that  $[\mathbf{Cp_2Co}]_2[\mathbf{1a}]$  is a diradical at room temperature. The isotropic exchange coupling extracted from the fit is -76 cm<sup>-1</sup>. Broken symmetry DFT calculations (vide infra) that predict J = -102 cm<sup>-1</sup> are consistent with these data.

## CYCLIC VOLTAMMETRY AND SPECTROELECTROCHEMISTRY

The cyclic voltammograms of 1a-1c collected in THF scanning from 0 V to -3 V featured four independent, quasi-reversible single-electron redox events (Table 1; Figure 3 and Figure S9). Unfortunately, the limited solubility of 1d precluded its analogous study. The Randles-Sevcik plots of 1a-1c (Figures S11-S13) display linearity and confirm that the redox events are diffusion-controlled. Scans swept in the anodic direction first were essentially identical and confirmed the independence of the observed redox events.

Based on the energy and reversibility of these redox events, we believe all four to be ligand-based. The first two quasireversible redox events  $(E_{1/2}(\mathbf{1}^{-/0}): -0.596 \text{ V}; E_{1/2}(\mathbf{1}^{2-/-}):$ -1.111 V) correspond to the sequential single electron addition to each ligand fragment, converting the monoanionic ligand to a dianionic radical (Scheme 5 and Figure S10). Similar processes were proposed for closely related group 10  $\beta$ dithioketonate derivatives  $M^{II}(S_2C_3RHR')_2$  (M = Ni, Pd, Pt; R/R' = alkyl, aryl). As supported by the solid-state structures of 1a and [Cp<sub>2</sub>Co]<sub>2</sub>[1a], we propose that addition of the first electron generates significant changes in the geometry of the chelate, which increases the energy required to reduce the second ligand. This barrier leads to two sequential singleelectron reductions rather than a single two-electron reduction. Similarly, the third and fourth redox events correspond to oneelectron processes to generate trianionic and tetranionic complexes, respectively (red in Figure S10). These four redox events were observed for 1a, 1b, and 1c (Table 1, Figure S9), where the potential at which the first two reduction events was found to be sensitive to the identity of the ligand parasubstituents (F, H, CH<sub>3</sub>; see Figure S9). As the electrondonating ability of the para-substituent increases (e.g., F < H < CH<sub>3</sub>), the reduction potentials decrease ( $\sim$ -100 mV shift from F to CH<sub>3</sub>).

Encouraged by the quasi-reversibility of the reduced species on the CV time scale (seconds to minutes), we pursued bulk electrolysis experiments to characterize the reduced products of 1a. Spectroelectrochemical studies were conducted on 1a in THF (0.5 mM) with  $[NBu_4][PF_6]$  (100 mM) as the supporting electrolyte using a standard H-cell (Figure S14). At an applied potential of -1.07 V vs Ag/Ag<sup>+</sup>, solutions of 1a gradually changed color from green to purple. During this time, 0.367 C were passed, consistent with quantitative conversion to a singly reduced product,  $1a^-$ . The doubly reduced product,  $1a^{2-}$  (dark brown), could be accessed from 1a at an applied potential of -1.49 V vs Ag/Ag<sup>+</sup> (0.552 C, Figure S15). Spectra of all three species are shown in Figure 4. Despite the quasi-

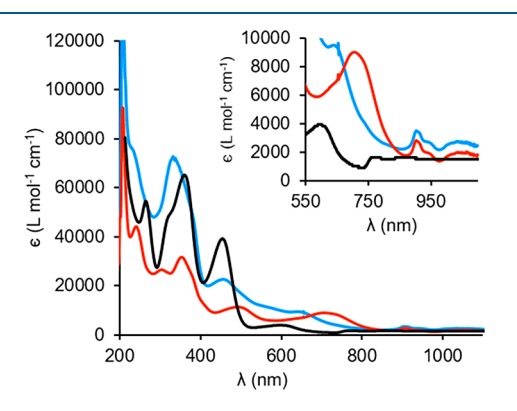


Figure 4. UV-vis spectra of 1a (black),  $1a^-$  (blue), and  $1a^{2-}$  (red) isolated from bulk electrolysis.

reversibility of the third and fourth reductions in the CV experiments, accessing these using bulk electrolysis proved challenging due to sample decomposition and instability of the solvent in the anodic compartment. To date, attempts to isolate samples of electrochemically generated  $1a^-$  and  $1a^{2-}$  free of working electrolyte have been unsuccessful due to the similar solubility properties of these species.

Electrochemically generated solutions of  $1a^-$  and  $1a^{2-}$  were further characterized by UV-vis and EPR spectroscopies.

While solutions of  $1a^-$  and  $1a^{2-}$  both appeared dark purple by eye, their electronic absorption spectra display features significantly shifted compared to 1a. This difference was most evident in the visible region of the absorption spectra (400-800 nm), where a clear red-shift was observed in the charge-transfer bands moving from 1a to  $1a^-$  and  $1a^{2-}$ . Similar red-shifting was observed for a series of homoleptic Pt(II) azoiminate complexes. In addition to the mentioned charge transfer bands, absorptions below 400 nm (e.g., intraligand  $\pi \to \pi^*$  transitions) were also sensitive to the oxidation state of 1a; however, no clear trend in peak energies for 1a,  $1a^-$ , and  $1a^{2-}$  was found.

No reversible oxidation features were observed in the oxidative direction up to  $\sim 1.0$  V. An irreversible feature was seen in each case at  $\sim 0.5$  V, which is currently under investigation. The sulfur-rich character of the HOMO (vide infra and Figure 5) and lack of reversibility may indicate intermolecular reactivity at S.

#### **■ EPR SPECTROSCOPY**

The EPR spectra of radicals found in group 10 complexes coordinated by bis-dithiolato/thiyl and similar ligands have been extensively documented over the past several decades. 7,27,69-75 In particular, Wieghardt, Yellowees, and coworkers have provided numerous examples of  $[M(L)_2]^{2-}$ ,  $[M(L)_2]^{1-}$ , and  $[M(L)_2]$  species.<sup>7,75–78</sup>  $[Pt(L)_2]^-$  radicals with significant metal-character often display rhombic (near axial) spectra with g-values significantly different than that of g<sub>e</sub> (e.g.,  $[Pt(L^{Bu})_2]^{1-}$ : g=2.21, 2.06, 1.80;  $L^{Bu}=3,5$ -di-tert-butylbenzene-1,2-dithiol). In contrast, ligand-centered radicals display g-values close to  $g_{\rm e}$  (2.0023) and often show hyperfine coupling to heteroatoms. EPR data collected of electrochemically generated 1a (Figures 6 and S16) support a doublet ground state with rhombic symmetry ( $g_1 = 2.007$ ,  $g_2 =$ 2.019,  $g_3 = 2.043$ ). Qualitatively, a small amount of hyperfine coupling was evident in the EPR spectrum of 1a; however, spectral resolution was insufficient to quantitatively resolve the low hyperfine coupling constants. The small g-shifting and minimal hyperfine coupling are consistent with a carbon- or sulfur-centered radical, while the anisotropic g-values point to partial radical delocalization to metal-based orbitals. These assignments are supported by the results of our DFT calculations on 1b-, which indicate small, but significant, contributions of Pt (2.7%) and N (1.0%) to the SOMO. As anticipated by the magnetometry data in Figure 2, the diradical species,  $[Cp_2Co]_2[1a]$ , is EPR silent at 77 K.

#### **■** DFT CALCULATIONS

Computational studies with hybrid functionals (details in the Supporting Information) of **1b** revealed that the  $\alpha$  HOMO is located largely on the {PtS<sub>4</sub>} core, and consistent with our experimental observations, the  $\alpha$  LUMO is based on the ligands with little metal contribution (Figure 5A,B). The {PtS<sub>4</sub>} core comprises 72% of the HOMO, while the thiocarbonyl groups contribute 69% to the LUMO, where orbital compositions are based on the CSPA partition (C-squared Population Analysis).

Upon reduction of **1b** to form **1b**<sup>-</sup>, the resulting electronic structure contains a SOMO (Figure 5C) largely localized on one of the bidentate ligands. Ligand backbone atoms account for 90% of the SOMO, while the Pt center contributes only 3%. The contribution of this chelate ring can be further

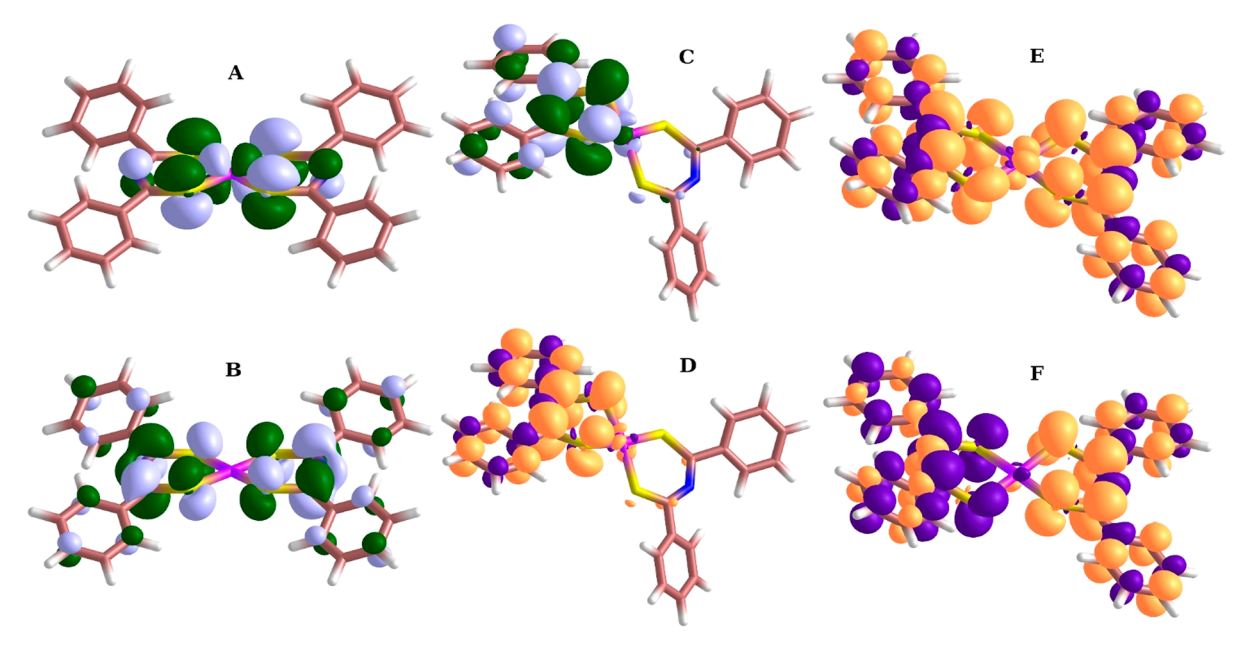
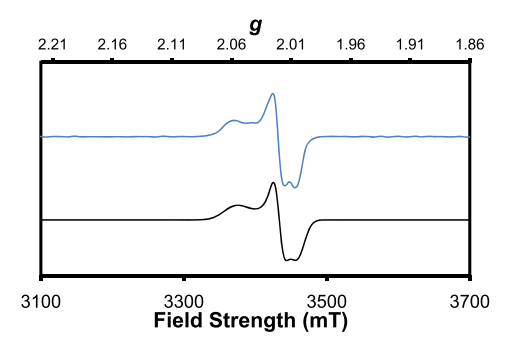


Figure 5. (A) HOMO of 1b; (B) LUMO of 1b; (C) SOMO of  $1b^-$ ; (D) spin density of  $1b^-$ ; (E) spin density for triplet state of  $1b^{2-}$ ; (F) spin density for broken symmetry solution of  $1b^{2-}$ .



**Figure 6.** X-band EPR spectrum of (nBu<sub>4</sub>N)[1a] (0.25 mM, blue line) in 1:1 THF/MeTHF collected at 77 K and simulated spectrum (black line; see the Supporting Information for further details).

decomposed into a composition of 0.8% from the nitrogen, 26% from sulfur, 30% from the thiocarbonyl carbons, and 35% from the phenyl rings.

Inspection of the spin density (Figure 5D) for 1b<sup>-</sup> and the SOMO composition listed above suggest that the thiocarbonyl

groups contain the bulk of the spin density. These thiocarbonyl groups polarize adjacent atoms, with the remaining atoms communicating via a spin polarization mechanism. Consistent with the EPR data of  $1a^-$  (Figure 6), there is little to no spin density found on N. Unfortunately, all attempts to isolate crystalline  $1a^-$  preparatively by chemical or electrochemical methods have proven unsuccessful.

Moving to  $1b^{2-}$ , the computations confirm the magnetization behavior shown in Figure 2, namely, an open-shell singlet ground state with an excited triplet state that is accessible at room temperature. The DFT-BS computed exchange coupling using Yamaguchi's formalism  $^{80,81}$  is -102 cm $^{-1}$ , which is in fair agreement with the experimental value of -76 cm $^{-1}$ .

The distinct bend seen between the  $\{PtS_4\}$  plane and each chelate ring upon reduction of 1b to  $[1b]^{1-}$  and to  $[1b]^{2-}$  in both the SCXRD and computational results is explained by the changes in the overlap of the chelate ring molecular orbitals with Pt, as shown in Scheme 6. As the ligand-based LUMOs each accept an additional electron, the S-C double bond

Scheme 7. Organic Compounds Related to the {cta<sup>R</sup>} Ligands

I, 
$$HctaPh^H$$

III,  $N$ -(pyridin-2-yl)benzothioamide

V, 2,4,6-triphenyl-1,3,5-dithiazine

S SR

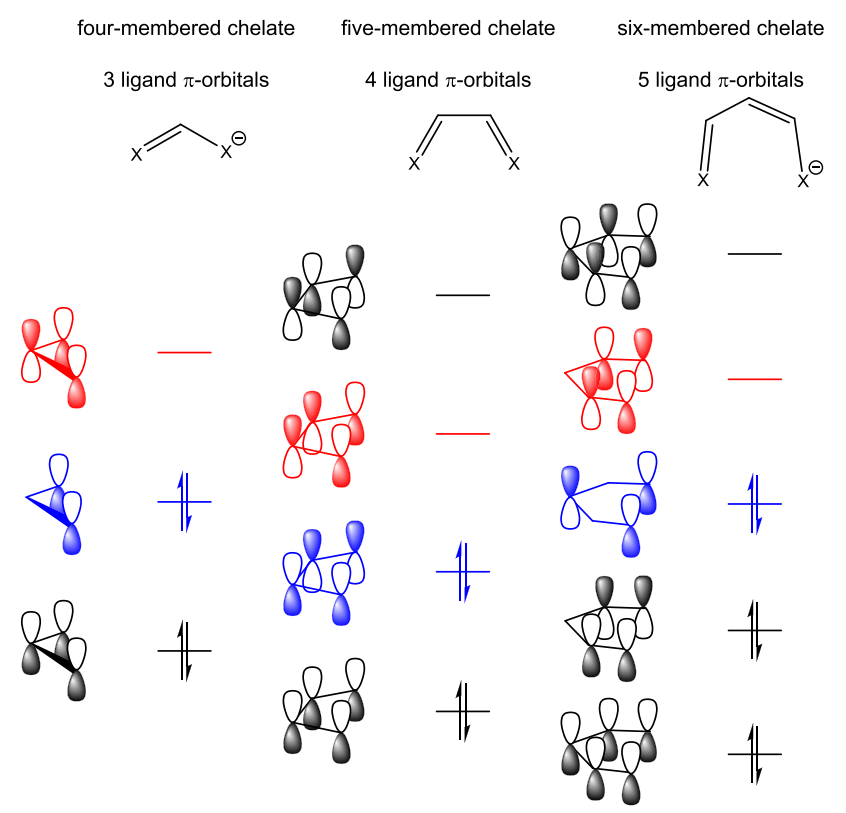
N

III,  $(ctaPh^H)_2$ 

IV, 3,5-diphenyl-1,2,4-dithiazolium

VI, Et( $ctaPh^H$ )

Scheme 8. Approximate Orbital Diagrams (Energy and Orbital Coefficients Not to Scale) for Chelating Ligands with Three, Four, and Five  $\pi$ -Type Orbitals<sup>a</sup>



<sup>a</sup>HOMOs are shown in blue, and LUMOs are shown in red.

character is lost, as shown in the middle of Scheme 4, and the increased S–C bond lengths (Figure S6). Therefore the S atoms are, formally, more  $sp^3$  than  $sp^2$  hybridized and lose  $\pi$  overlap with Pt  $d_{xz}/d_{yz}$ . The chelate ring LUMO in neutral 1 is orthogonal to the empty Pt  $d_{x^2-y^2}$ , as shown in the top of Scheme 6, but gains  $\sigma$  overlap upon reduction and bending, as shown at the bottom. Furthermore, this increased interaction of the two singly occupied  $\pi$  systems on the two chelate rings with the  $d_{x^2-y^2}$  orbital provides a direct exchange pathway for the AF coupling described above. The calculated energies for the antiferromagnetic coupling as a function of a bend angle are shown in Figure S23 and clearly indicate increased coupling with increased bending.

## DISCUSSION

It is striking that the thiobenzamide moiety has received little mention in the literature. There are only a handful of related organic moieties derived from thiobenzamide, as shown in Scheme 7. A 1979 patent describes a series of thioaroylarylthiocarboxylic acid amides and their disulfides, II,82 but only one subsequent publication mentions these compounds.<sup>83</sup> Thioamides with 2-pyridyl substituents, III, have been investigated for lubricating oils.<sup>84</sup> The most abundant and closely related organic compounds to HctaPh are the 1,2,4-dithiazolium salts, IV, of which several symmetric and asymmetric 3,5-diaryl species are known.85 Compounds with a six-membered 1,3,5dithiazine ring, V, are also known.86 In our study, we have demonstrated that this organic moiety is easily formed under mild conditions using simple and widely available precursors (e.g., bicarbonate, thiobenzamide, and metal salts). To the best of our knowledge, the synthesis of 1a-1d marks the first

examples of metal complexes containing the condensed thio amide,  $\mathsf{HctaPh}^\mathsf{H},\,\mathbf{I}.$ 

A survey of the organic literature strongly suggests that the free  $\operatorname{HctaPh}^R$  ligands would be highly susceptible to oxidation to form an intra- or intermolecular disulfide bond. Consistent with these expectations, attempts to isolate free  $\operatorname{H}(\operatorname{cta}^{\operatorname{Ph}})$  via protonation of  $\operatorname{1a-1d}$ , even with strong mineral acids, failed to generate stable  $\operatorname{H}(\operatorname{cta}^{\operatorname{Ph}})$ . The inability to access free  $\operatorname{H}(\operatorname{cta}^{\operatorname{Ph}})$  is comparable to  $\operatorname{HSacSac}$ , the unstable sulfur analogue of the ubiquitous and commercially available acetylacetone ligand,  $\operatorname{Hacac}$ . Few derivatives have been reported, but a  $\operatorname{Pd}$  dithio- $\beta$ -diketonate complex with  $\operatorname{tert}$ -butyl substitution,  $[\operatorname{Pd}(\operatorname{S,S-tmhd})_2]$  ( $\operatorname{tmhd} = \operatorname{tetramethyl-3,S-heptanedithione}$ ), has been structurally characterized, and the ligand-centered electrochemistry of these complexes has been predicted and subsequently reported. Alkylated versions, the thioethers  $\operatorname{R}(\operatorname{cta}^{\operatorname{Ph}})$ ,  $\operatorname{VI}$ , have been prepared and characterized.

One early proposal for the initial lack of redox-active six-membered chelate rings came from Schrauzer<sup>89</sup> who suggested that an odd number of  $\pi$ -type ligand orbitals favored only a singly reduced redox state. This argument was qualitative and was based on the perceived relative energetic differences between HOMO and LUMO for each of the three common chelate ligand ring sizes. Three common chelate ring sizes of potential redox-active ligands are shown in Scheme 8 along with representations of their ligand  $\pi$ -type molecular orbitals, with the  $\pi$  electrons filled in accord with closed shell ligand configurations. Another way to classify chelating redox-active ligands is not only in terms of the number of atoms in the chelate ring but alternatively in the number of p-block atoms whose  $\pi$ - and  $\pi$ \*-type orbitals are the basis of the redox

activity. From this point of view, a six-membered chelate ring contains five p-block elements that participate in a  $\pi$ -bonding system. Schrauzer argued that the HOMO–LUMO gap in the "odd" systems, four- and six-membered chelate rings that had three and five  $\pi$ -type orbitals, respectively, was too great to allow ligand reduction for monoanionic ligands such as acetylacetonate. <sup>89</sup>

As became evident in the 1960s, adding one or more electrons to a neutral dithiolene, ortho-quinone, or diazadiene five-membered chelate ring (four  $\pi$ -type orbitals in XCCX ligand, X = donor heteroatom, Scheme 8) caused lengthening of the X–C bonds (X = p-block donor atom) and shortening of the central C–C bond as the former increased in single-bond character and the latter in double-bond character. Both changes are consistent with increasing occupation of the red LUMO in the center of Scheme 8. Thus, changes in intraligand bond distances are a strong indicator of ligand redox changes. The lack of distance changes, however, does not guarantee a lack of reactivity.

More recently, the importance of where the nodes are in redox-active orbitals was emphasized. The complex [Ni-(nacnac)<sub>2</sub>], mentioned above and in Scheme 1, can be oxidized, and the electron comes from a XCCCX ligand-based orbital, as shown in blue on the right-hand side of Scheme 8. That ligand HOMO displays neither strongly bonding or antibonding character and leads to minimal changes in any of the intraligand bond distances in [Ni(nacnac)<sub>2</sub>]<sup>+</sup>. For ligand electronic structure changes to be detected by single-crystal X-ray diffraction, there must be significant bonding character in orbitals from which electrons are removed or significant antibonding character for orbitals that are newly occupied.

Therefore, it is now clear that if the redox-active orbital is neither significantly bonding nor significantly antibonding, a change in its occupation will not be detectable by SCXRD. Such is the case for oxidation of a six-membered chelate ring, because the ligand HOMO (blue, at the right in Scheme 8) displays neither strong bonding or antibonding character, similar to that described for  $[Ni(nacnac)_2]^{+,90}$  In contrast, reduction of such a six-membered ring, as in the case of  $[Pt(ctaPh^R)_2]$ , does bring about structurally demonstrable changes because occupation of the LUMO (red, at the right in Scheme 8) decreases the S–C bond order, as observed in the crystal structure changes upon reduction of 1a to  $[Cp_2Co]_2[1a]$ .

Based on the foregoing work, we can see that both the orbital energy and bonding character in potentially redoxactive ligands play a role in whether or not electron transfer takes place. For a ligand to be redox active in a reductive sense, it must have an empty ligand orbital lower than any metal-based orbital. Likewise, for a ligand to be oxidized, its occupied orbitals must be higher than any metal ones. It is not the size of the chelate ring that determines hidden redox-active ligand character but the electronic structure of the redox-active orbital. Depending on the particular complex, oxidation or reduction of the ligand might lead to a stable species. Even when monoanionic ligands are oxidized to neutral ones, their Lewis basic nature and chelating character can keep them bound to a metal center.<sup>27</sup>

The four single electron reduction events observed for 1a-1d are entirely consistent with this picture. The electronic structure of the dianionic radical shown on the right-hand side in Scheme 5 places the unpaired electron density on the C atoms of the ring, consistent with EPR data and DFT

calculations above. This dianion has less C=S double-bond character than the monoanion, consistent with the C-S bond lengthening seen between 1a and  $[Cp_2Co]_2[1a]$ . Other resonance structures that place the radical character on the central atom of the six-membered chelate ring, based on possible allowed Lewis structures, have been proposed.<sup>20</sup>

Redox-active six-membered chelate rings have been less often seen to date because the  $\pi^*$  orbitals into which electrons would go are not the LUMOs of the molecules bearing such ligands. Two mechanisms to make the  $\pi^*$  orbitals the LUMOs have been demonstrated in extant examples: (i) substituents with extended  $\pi$  systems that can accommodate additional electrons  $^{23,26,29,30,32,33}$  or (ii) additional ligands that force a change in coordination number and drive metal orbital energies below those of ligand LUMOs and facilitate ligand reduction. Herein, we report a third and potentially more general approach. When the donor atoms are S, and not O or N, the  $\pi^*$  orbitals are lower in energy and sufficiently so as to accept electrons, as we have now observed in the  $\{Pt(cta)_2\}$  system.

#### CONCLUSIONS

A new template condensation reaction has been discovered leading to four Pt(II) complexes of the general form  $[Pt(ctaPh^R)_2]$ , R = CH<sub>3</sub> (1a), H (1b), F (1c), Cl (1d), cta =  $\underline{c}$  ondensed  $\underline{t}$  hio $\underline{a}$  mide. The ligand is redox active and can be reduced from the initial monoanion to a dianionic and then trianionic state. A singly reduced species, [1a]<sup>1-</sup>, containing [Pt(ctaPh<sup>CH3</sup>)<sub>2</sub>]<sup>1-</sup> has been generated in situ and characterized by UV-vis and EPR spectroscopies. A doubly reduced species  $[Cp_2Co]_2[Pt(ctaPh^{CH3})_2]$ ,  $[Cp_2Co]_2[1a]$ , was prepared, isolated, and shown to have, in the solid state, a singlet ground state and triplet excited state with  $J = -76 \text{ cm}^{-1}$ . DFT studies of 1b, [1b]<sup>1-</sup>, and [1b]<sup>2-</sup> confirm the location of additional electrons in exclusively ligand-based orbitals. These studies and prior work in the literature demonstrate that several different molecular factors can favor redox-active ligands. Compared to O- and N-donor ligands, the  $\pi^*$  orbitals of S-donor ones are lower than empty metal-based orbitals and can favor redoxactive ligands, if alternative S-based redox chemistry does not interfere.

#### ASSOCIATED CONTENT

## Supporting Information

The Supporting Information is available free of charge at https://pubs.acs.org/doi/10.1021/acs.inorgchem.1c01693.

X-ray diffraction collection parameters, selected metrical data, ORTEPs of 1a, 1c, and 1d, UV-vis and EPR spectroscopic, electrochemical, and magnetic data as well as computational details (PDF)

#### **Accession Codes**

CCDC 2074905–2074909 contain the supplementary crystallographic data for this paper. These data can be obtained free of charge via www.ccdc.cam.ac.uk/data\_request/cif, or by emailing data\_request@ccdc.cam.ac.uk, or by contacting The Cambridge Crystallographic Data Centre, 12 Union Road, Cambridge CB2 1EZ, UK; fax: +44 1223 336033.

## AUTHOR INFORMATION

#### **Corresponding Author**

Linda H. Doerrer – Department of Chemistry, Boston University, Boston, Massachusetts 02215, United States;

orcid.org/0000-0002-2437-6374; Email: doerrer@bu.edu

#### **Authors**

Linda A. Zuckerman – Department of Chemistry, Boston University, Boston, Massachusetts 02215, United States Natasha P. Vargo – Department of Chemistry, Brown University, Providence, Rhode Island 02912, United States

Claire V. May – Department of Chemistry, Boston University, Boston, Massachusetts 02215, United States

Michael P. Crockett – Department of Chemistry, Boston College, Chestnut Hill, Massachusetts 02467, United States Ariel S. Hyre – Department of Chemistry, Boston University, Boston, Massachusetts 02215, United States

James McNeely — Department of Chemistry, Boston University, Boston, Massachusetts 02215, United States Jessica K. Elinburg — Department of Chemistry, Boston University, Boston, Massachusetts 02215, United States; orcid.org/0000-0003-3064-3771

Alexander M. Brown — Department of Chemistry, Brown University, Providence, Rhode Island 02912, United States Jerome R. Robinson — Department of Chemistry, Brown University, Providence, Rhode Island 02912, United States; orcid.org/0000-0002-9111-3822

Arnold L. Rheingold — Department of Chemistry and Biochemistry, University of California, San Diego, La Jolla, California 92093, United States; orcid.org/0000-0003-4472-8127

Complete contact information is available at: https://pubs.acs.org/10.1021/acs.inorgchem.1c01693

#### Notes

The authors declare no competing financial interest.

#### ACKNOWLEDGMENTS

We thank Dr. Rebecca Loy for helpful discussions and NSF-LHD (CHE 01800313), NSF-NMR (CHE 0619339), UROP (L.A.Z. and C.V.M.), and NSF-GRFP (A.S.H.) for financial support. We thank Dr. Majed Fataftah for assistance in fitting the magnetic data, Prof. Odile Eisenstein (CNRS, Université de Montpellier, France) for thoughtful discussions, and Prof. Michael Graf (Department of Physics, Boston College) for access to the SQUID magnetometer who thank the NSF for the instrument (DMR 1337567). J.R.R. gratefully acknowledges the NSF (CHE-1900248) and Brown University (start-up) for financial support of this work.

## **■** REFERENCES

- (1) Stiefel, E. I. Dithiolene Chemistry; Wiley: 2004; p 583, DOI: 10.1002/0471471933.ch10.
- (2) McCleverty, J. A. Metal 1,2-dithiolene and related complexes. *Prog. Inorg. Chem.* **2007**, *10*, 49–221.
- (3) Pierpont, C. G. Unique properties of transition metal quinone complexes of the MQ3 series. *Coord. Chem. Rev.* **2001**, 219–221, 415–433.
- (4) Klein, R. A.; Elsevier, C. J.; Hartl, F. Redox Properties of Zerovalent Palladium Complexes Containing  $\alpha$ -Diimine and p-Quinone Ligands. *Organometallics* **1997**, *16* (6), 1284–1291.
- (5) Broere, D. L. J.; Plessius, R.; van der Vlugt, J. I. New avenues for ligand-mediated processes expanding metal reactivity by the use of redox-active catechol, o-aminophenol and o-phenylenediamine ligands. *Chem. Soc. Rev.* **2015**, 44 (19), 6886–6915.

- (6) Mukherjee, R. Assigning Ligand Redox Levels in Complexes of 2-Aminophenolates: Structural Signatures. *Inorg. Chem.* **2020**, 59 (18), 12961–12977.
- (7) Chaudhuri, P.; Verani, C. N.; Bill, E.; Bothe, E.; Weyhermüller, T.; Wieghardt, K. Electronic Structure of Bis(o-iminobenzosemiquinonato)metal Complexes (Cu, Ni, Pd). The Art of Establishing Physical Oxidation States in Transition-Metal Complexes Containing Radical Ligands. J. Am. Chem. Soc. 2001, 123 (10), 2213–2223.
- (8) Bart, S. C.; Chlopek, K.; Bill, E.; Bouwkamp, M. W.; Lobkovsky, E.; Neese, F.; Wieghardt, K.; Chirik, P. J. Electronic Structure of Bis(imino)pyridine Iron Dichloride, Monochloride, and Neutral Ligand Complexes: A Combined Structural, Spectroscopic, and Computational Study. *J. Am. Chem. Soc.* **2006**, *128* (42), 13901–13912.
- (9) Roemelt, C.; Weyhermueller, T.; Wieghardt, K. Structural characteristics of redox-active pyridine-1,6-diimine complexes: Electronic structures and ligand oxidation levels. *Coord. Chem. Rev.* **2019**, 380, 287–317.
- (10) Ganguly, S.; Ghosh, A. Seven Clues to Ligand Noninnocence: The Metallocorrole Paradigm. *Acc. Chem. Res.* **2019**, *52*, 2003.
- (11) van der Vlugt, J. I. Radical-Type Reactivity and Catalysis by Single-Electron Transfer to or from Redox-Active Ligands. *Chem. Eur. J.* **2019**, 25 (11), 2651–2662.
- (12) de Bruin, B.; Gualco, P.; Paul, N. D. Redox Non-innocent Ligands. In *Ligand Design in Metal Chemistry*; Wiley-Blackwell: 2016; pp 176–204, DOI: 10.1002/9781118839621.ch7.
- (13) Mingos, D. M. P. A review of complexes of ambivalent and ambiphilic Lewis acid/bases with symmetry signatures and an alternative notation for these non-innocent ligands. *J. Organomet. Chem.* **2014**, *751*, 153–173.
- (14) Adarsh, N. N.; Dastidar, P. Coordination polymers: what has been achieved in going from innocent 4,4'-bipyridine to bis-pyridyl ligands having a non-innocent backbone? *Chem. Soc. Rev.* **2012**, *41* (8), 3039–3060.
- (15) Kaim, W. The Shrinking World of Innocent Ligands: Conventional and Non-Conventional Redox-Active Ligands. *Eur. J. Inorg. Chem.* **2012**, 2012 (3), 343–348.
- (16) Lyaskovskyy, V.; de Bruin, B. Redox Non-Innocent Ligands: Versatile New Tools to Control Catalytic Reactions. *ACS Catal.* **2012**, 2 (2), 270–279.
- (17) Kaim, W.; Schwederski, B. Non-innocent ligands in bioinorganic chemistry: An overview. *Coord. Chem. Rev.* **2010**, 254 (13–14), 1580–1588.
- (18) van der Vlugt, J. I.; Reek, J. N. H. Neutral Tridentate PNP Ligands and Their Hybrid Analogs: Versatile Non-Innocent Scaffolds for Homogeneous Catalysis. *Angew. Chem., Int. Ed.* **2009**, 48 (47), 8832–8846.
- (19) Queyriaux, N. Redox-Active Ligands in Electroassisted Catalytic H+ and CO2 Reductions: Benefits and Risks. *ACS Catal.* **2021**, *11* (7), 4024–4035.
- (20) Kaim, W. Chelate rings of different sizes with non-innocent ligands. *Dalton Trans.* **2019**, 48 (24), 8521–8529.
- (21) Vinum, M. G.; Voigt, L.; Hansen, S. H.; Bell, C.; Clark, K. M.; Larsen, R. W.; Pedersen, K. S. Ligand field-actuated redox-activity of acetylacetonate. *Chem. Sci.* **2020**, *11* (31), 8267–8272.
- (22) Vinum, M. G.; Voigt, L.; Bell, C.; Mihrin, D.; Larsen, R. W.; Clark, K. M.; Pedersen, K. S. Evidence for Non-Innocence of a  $\beta$ -Diketonate Ligand. *Chem. Eur. J.* **2020**, 26 (10), 2143–2147.
- (23) Das, A.; Scherer, T. M.; Mobin, S. M.; Kaim, W.; Lahiri, G. K. 9-Oxidophenalenone: A Noninnocent  $\beta$ -Diketonate Ligand? *Inorg. Chem.* **2012**, *51* (7), 4390–4397.
- (24) Hazari, A. S.; Paretzki, A.; Fiedler, J.; Zalis, S.; Kaim, W.; Lahiri, G. K. Different manifestations of enhanced  $\pi$ -acceptor ligation at every redox level of [Os(9-OP)L2]n, n = 2+, +, 0, (9-OP-= 9-oxidophenalenone and L = bpy or pap). Dalton Trans. **2016**, 45 (45), 18241–18251.
- (25) Bhunia, M.; Sahoo, S. R.; Shaw, B. K.; Vaidya, S.; Pariyar, A.; Vijaykumar, G.; Adhikari, D.; Mandal, S. K. Storing redox equivalent

- in the phenalenyl backbone towards catalytic multi-electron reduction. *Chem. Sci.* **2019**, *10* (31), 7433–7441.
- (26) Storr, T.; Wasinger, E. C.; Pratt, R. C.; Stack, T. D. P. The Geometric and Electronic Structure of a One-Electron-Oxidized Nickel(II) Bis(salicylidene)diamine Complex. *Angew. Chem., Int. Ed.* **2007**, *46* (27), 5198–5201.
- (27) Khusniyarov, M. M.; Bill, E.; Weyhermuller, T.; Bothe, E.; Wieghardt, K. Hidden noninnocence: theoretical and experimental evidence for redox activity of a  $\beta$ -diketiminate1- ligand. *Angew. Chem., Int. Ed.* **2011**, 50 (7), 1652–5.
- (28) Cowley, R. E.; Christian, G. J.; Brennessel, W. W.; Neese, F.; Holland, P. L. A Reduced ( $\beta$ -Diketiminato)iron Complex with End-On and Side-On Nitriles: Strong Backbonding or Ligand Non-Innocence? *Eur. J. Inorg. Chem.* **2012**, 2012 (3), 479–483.
- (29) Camp, C.; Arnold, J. On the non-innocence of "Nacnacs": ligand-based reactivity in  $\beta$ -diketiminate supported coordination compounds. *Dalton Trans.* **2016**, 45 (37), 14462–14498.
- (30) King, E. R.; Betley, T. A. C-H Bond Amination from a Ferrous Dipyrromethene Complex. *Inorg. Chem.* **2009**, 48 (6), 2361–2363.
- (31) Locher, J.; Watt, F. A.; Neuba, A. G.; Schoch, R.; Munz, D.; Hohloch, S. Molybdenum(VI) bis-imido Complexes of Dipyrromethene Ligands. *Inorg. Chem.* **2020**, *59* (14), 9847–9856.
- (32) Oakley, S. R.; Nawn, G.; Waldie, K. M.; MacInnis, T. D.; Patrick, B. O.; Hicks, R. G. Nindigo": synthesis, coordination chemistry, and properties of indigo diimines as a new class of functional bridging ligands. *Chem. Commun.* **2010**, 46 (36), 6753–6755.
- (33) Fortier, S.; Moral, O. G.-d.; Chen, C.-H.; Pink, M.; Le Roy, J. J.; Murugesu, M.; Mindiola, D. J.; Caulton, K. G. Probing the redox non-innocence of dinuclear, three-coordinate Co(ii) nindigo complexes: not simply  $\beta$ -diketiminate variants. *Chem. Commun.* **2012**, 48 (90), 11082–11084.
- (34) Chang, M.-C.; McNeece, A. J.; Hill, E. A.; Filatov, A. S.; Anderson, J. S. Ligand-Based Storage of Protons and Electrons in Dihydrazonopyrrole Complexes of Nickel. *Chem. Eur. J.* **2018**, 24 (31), 8001–8008.
- (35) Bauer, S.; Záliš, S.; Fiedler, J.; Ringenberg, M. R.; Kaim, W. Oxidation State Assignments in the Organoplatinum One-Electron Redox Series [(NN)PtMes2]n, n = + ,0, ,2. Eur. J. Inorg. Chem. **2020**, 2020 (25), 2435–2443.
- (36) Chang, M.-C.; Dann, T.; Day, D. P.; Lutz, M.; Wildgoose, G. G.; Otten, E. The Formazanate Ligand as an Electron Reservoir: Bis(Formazanate) Zinc Complexes Isolated in Three Redox States. *Angew. Chem., Int. Ed.* **2014**, 53 (16), 4118–4122.
- (37) Ghosh, S.; Rana, S.; Kabir, S. E.; Richmond, M. G.; Hogarth, G. Highly efficient electrocatalytic proton-reduction by coordinatively and electronically unsaturated  $Fe(CO)(\kappa 2\text{-dppn})(\kappa 2\text{-tdt})$ . *Inorg. Chim. Acta* **2019**, 486, 435–440.
- (38) Bousman, K. S.; Toscano, P. J.; Welch, J. T. The effect of sulfur on CVD performance of Pd(II)  $\beta$ -diketonate precursors and the completion of a structural trans-influence series: synthesis and structural characterization of Pd(S,S-tmhd)2. *Inorg. Chim. Acta* **2004**, 357 (13), 3871–3876.
- (39) Boyd, P. D. W.; Rickard, C. E. F.; Cavell, K. J. [Bis-diphenylphosphino)alkane](pentane-2,4-dithionato) complexes of nickel(II). *Acta Crystallogr., Sect. C: Cryst. Struct. Commun.* **2000**, C56 (1), e16–e18.
- (40) Boyd, P. D. W.; Hope, J.; Martin, R. L. Synthesis and properties of tris(dithioacetylacetonato)vanadium(III). *J. Chem. Soc., Dalton Trans.* 1986, No. 4, 887–9.
- (41) Bowmaker, G. A.; Boyd, P. D. W.; Zvagulis, M.; Cavell, K. J.; Masters, A. F. Electron spin resonance studies of the one-electron-reduction products of nickel(II) 1,3-dithio  $\beta$ -diketonate complexes. *Inorg. Chem.* **1985**, 24 (3), 401–8.
- (42) Beach, S. A.; Doerrer, L. H. Heterobimetallic Lantern Complexes and Their Novel Structural and Magnetic Properties. *Acc. Chem. Res.* **2018**, *51* (5), 1063–1072.
- (43) Nimthong-Roldan, A.; Guillet, J. L.; McNeely, J.; Ozumerzifon, T. J.; Shores, M. P.; Golen, J. A.; Rheingold, A. L.; Doerrer, L. H.

- Quasi-1D chains of dinickel lantern complexes and their magnetic properties. *Dalton Trans.* **2017**, *46* (17), 5546–5557.
- (44) Baddour, F. G.; Hyre, A. S.; Guillet, J. L.; Pascual, D.; Lopez-de-Luzuriaga, J. M.; Alam, T. M.; Bacon, J. W.; Doerrer, L. H. Pt-Mg, Pt-Ca, and Pt-Zn Lantern Complexes and Metal-Only Donor-Acceptor Interactions. *Inorg. Chem.* **2017**, *56* (1), 452–469.
- (45) Guillet, J. L.; Bhowmick, I.; Shores, M. P.; Daley, C. J. A.; Gembicky, M.; Golen, J. A.; Rheingold, A. L.; Doerrer, L. H. Thiocyanate-Ligated Heterobimetallic {PtM} Lantern Complexes Including a Ferromagnetically Coupled 1D Coordination Polymer. *Inorg. Chem.* **2016**, *55* (16), 8099–8109.
- (46) Baddour, F. G.; Fiedler, S. R.; Shores, M. P.; Golen, J. A.; Rheingold, A. L.; Doerrer, L. H. Heterobimetallic Lantern Complexes That Couple Antiferromagnetically through Noncovalent Pt···Pt Interactions. *Inorg. Chem.* **2013**, 52 (9), 4926–4933.
- (47) Baddour, F. G.; Fiedler, S. R.; Shores, M. P.; Bacon, J. W.; Golen, J. A.; Rheingold, A. L.; Doerrer, L. H. Pt···Pt vs. Pt···S Contacts Between Pt-Containing Heterobimetallic Lantern Complexes. *Inorg. Chem.* **2013**, *52* (23), 13562–13575.
- (48) Dahl, E. W.; Baddour, F. G.; Fiedler, S. R.; Hoffert, W. A.; Shores, M. P.; Yee, G. T.; Djukic, J.-P.; Bacon, J. W.; Rheingold, A. L.; Doerrer, L. H. Antiferromagnetic coupling across a tetrametallic unit through noncovalent interactions. *Chem. Sci.* **2012**, *3* (2), 602–609.
- (49) Bonde, N. A.; Petersen, J. B.; Sørensen, M. A.; Nielsen, U. G.; Fåk, B.; Rols, S.; Ollivier, J.; Weihe, H.; Bendix, J.; Perfetti, M. Importance of Axial Symmetry in Elucidating Lanthanide—Transition Metal Interactions. *Inorg. Chem.* **2020**, *59* (1), 235–243.
- (50) Soerensen, M. A.; Hansen, U. B.; Perfetti, M.; Pedersen, K. S.; Bartolome, E.; Simeoni, G. G.; Mutka, H.; Rols, S.; Jeong, M.; Zivkovic, I.; Retuerto, M.; Arauzo, A.; Bartolome, J.; Piligkos, S.; Weihe, H.; Doerrer, L. H.; van Slageren, J.; Roennow, H. M.; Lefmann, K.; Bendix, J. Chemical tunnel-splitting-engineering in a dysprosium-based molecular nanomagnet. *Nat. Commun.* **2018**, 9 (1), 1292.
- (51) Soerensen, M. A.; Weihe, H.; Vinum, M. G.; Mortensen, J. S.; Doerrer, L. H.; Bendix, J. Imposing high-symmetry and tuneable geometry on lanthanide centres with chelating Pt and Pd metalloligands. *Chem. Sci.* **2017**, *8* (5), 3566–3575.
- (52) Dolinar, B. S.; Kozimor, S. A.; Berry, J. F. K3[Mo2(SNO5)-4Cl]3[Mo2(SNO5)4]: the first example of a heterometallic extended metal atom node (HEMAN). *Dalton Trans.* **2016**, 45 (44), 17602–17605.
- (53) Dolinar, B. S.; Berry, J. F. Influence of Lewis acid charge and proximity in MoMo···M linear chain compounds with M = Na+, Ca2+, Sr2+, and Y3+. Polyhedron **2016**, 103, 71–78.
- (54) Dolinar, B. S.; Berry, J. F. Lewis Acid Enhanced Axial Ligation of [Mo2]4+ Complexes. *Inorg. Chem.* **2013**, 52 (8), 4658–4667.
- (55) Wächtler, E.; Oro, L. A.; Iglesias, M.; Gerke, B.; Pöttgen, R.; Gericke, R.; Wagler, J. Synthesis and Oxidation of a Paddlewheel-Shaped Rhodium/Antimony Complex Featuring Pyridine-2-Thiolate Ligands. *Chem. Eur. J.* **2017**, 23 (14), 3447–3454.
- (56) Scott, T. A.; Abbaoui, B.; Zhou, H.-C. Crystallographic Evidence for Chromium-Platinum Interaction. *Inorg. Chem.* **2004**, 43 (8), 2459–2461.
- (57) Kitano, K. i.; Tanaka, R.; Kimura, T.; Tsuda, T.; Shimizu, S.; Takagi, H.; Nishioka, T.; Shiomi, D.; Ichimura, A.; Kinoshita, I.; Isobe, K.; Ooi, S. i. Lantern-type dinuclear CrIIIPtII and VIVPtII complexes bridged by pyridine-2-thiolate. Synthesis and characterization. *J. Chem. Soc., Dalton Trans.* **2000**, No. 6, 995–1000.
- (58) Kitano, K. i.; Tanaka, K.; Nishioka, T.; Ichimura, A.; Kinoshita, I.; Isobe, K.; Ooi, S. i. Lantern type heterobimetallic complexes. Tetra-ε-4-methylpyridine-2-thiolato bridged platinum(II)cobalt(II) and oxidation complexes †. *J. Chem. Soc., Dalton Trans.* **1998**, No. 19, 3177–3182.
- (59) Lifsey, R. S.; Chavan, M. Y.; Chau, L. K.; Ahsan, M. Q.; Kadish, K. M.; Bear, J. L. Dirhodium complexes with axially and equatorially nonequivalent rhodium atoms. Characterization of Rh2(tcl)4(tclH) and Rh2(tcl)4(CO) (tcl = .omega.-thiocaprolactamate). *Inorg. Chem.* 1987, 26 (6), 822–829.

- (60) Groom, C. R.; Bruno, I. J.; Lightfoot, M. P.; Ward, S. C. The Cambridge Structural Database. *Acta Crystallogr., Sect. B: Struct. Sci., Cryst. Eng. Mater.* **2016**, 72 (2), 171–179.
- (61) Yang, L.; Powell, D. R.; Houser, R. P. Structural variation in copper(i) complexes with pyridylmethylamide ligands: structural analysis with a new four-coordinate geometry index, τ4. *Dalton Trans.* **2007**, No. 9, 955–964.
- (62) Huheey, J. E.; Keiter, E. A.; Keiter, R. L. Inorganic Chemistry, 4th ed.; Harper Collins: 1993; p 964.
- (63) Doerrer, L. H. Steric and electronic effects in metallophilic double salts. *Dalton Trans.* **2010**, 39 (15), 3543–3553.
- (64) Shupack, S. I.; Billig, E.; Clark, R. J. H.; Williams, R.; Gray, H. B. The Electronic Structures of Square-Planar Metal Complexes. V. Spectral Properties of the Maleonitriledithiolate Complexes of Nickel, Palladium, and Platinum. *J. Am. Chem. Soc.* **1964**, *86* (21), 4594–4602
- (65) Chilton, N. F.; Anderson, R. P.; Turner, L. D.; Soncini, A.; Murray, K. S. PHI: A powerful new program for the analysis of anisotropic monomeric and exchange-coupled polynuclear d- and f-block complexes. *J. Comput. Chem.* **2013**, *34* (13), 1164–1175.
- (66) Zanello, P. Inorganic Electrochemistry; Royal Society of Chemistry: 2003; p 615, DOI: 10.1039/9781847551146.
- (67) Heath, G. A.; Leslie, J. H. Redox-active planar complexes. Electrochemical investigations of palladium and platinum bis-(dithioacetylacetonate) complexes and their structural analogs. *J. Chem. Soc., Dalton Trans.* 1983, No. 8, 1587–92.
- (68) Mu, G.; Cong, L.; Wen, Z.; Wu, J. I. C.; Kadish, K. M.; Teets, T. S. Homoleptic Platinum Azo-iminate Complexes via Hydrogenative Cleavage of Formazans. *Inorg. Chem.* **2018**, *57* (15), 9468–9477.
- (69) Arumugam, K.; Selvachandran, M.; Obanda, A.; Shaw, M. C.; Chandrasekaran, P.; Caston Good, S. L.; Mague, J. T.; Sproules, S.; Donahue, J. P. Redox-Active Metallodithiolene Groups Separated by Insulating Tetraphosphinobenzene Spacers. *Inorg. Chem.* **2018**, *57* (7), 4023–4038.
- (70) Mews, N. M.; Reimann, M.; Hörner, G.; Kaupp, M.; Schubert, H.; Berkefeld, A. A four-parameter system for rationalising the electronic properties of transition metal—radical ligand complexes. *Dalton Transactions* **2020**, *49* (28), 9735–9742.
- (71) Bélombé, M. M.; Nenwa, J.; Hey-Hawkins, E.; Lönnecke, P.; Strauch, P.; Koch, K. R. Synthesis, EPR spectrum and X-ray structure of tetra-n-butylammonium bis(benzene-1,2-dithiolato(2-)-κ2S,S')-platinate(III). *Polyhedron* **2008**, 27 (18), 3688–3692.
- (72) Loughrey, J. J.; Patmore, N. J.; Baldansuren, A.; Fielding, A. J.; McInnes, E. J. L.; Hardie, M. J.; Sproules, S.; Halcrow, M. A. Platinum(ii) complexes of mixed-valent radicals derived from cyclotricatechylene, a macrocyclic tris-dioxolene. *Chem. Sci.* **2015**, 6 (12), 6935–6948.
- (73) Broere, D. L. J.; de Bruin, B.; Reek, J. N. H.; Lutz, M.; Dechert, S.; van der Vlugt, J. I. Intramolecular Redox-Active Ligand-to-Substrate Single-Electron Transfer: Radical Reactivity with a Palladium(II) Complex. J. Am. Chem. Soc. 2014, 136 (33), 11574—11577.
- (74) Shavaleev, N. M.; Davies, E. S.; Adams, H.; Best, J.; Weinstein, J. A. Platinum(II) Diimine Complexes with Catecholate Ligands Bearing Imide Electron-Acceptor Groups: Synthesis, Crystal Structures, (Spectro)Electrochemical and EPR studies, and Electronic Structure. *Inorg. Chem.* 2008, 47 (5), 1532–1547.
- (75) Pap, J. S.; Benedito, F. L.; Bothe, E.; Bill, E.; DeBeer George, S.; Weyhermüller, T.; Wieghardt, K. Dimerization Processes of Square Planar [PtII(tbpy)(dithiolato●)]+ Radicals. *Inorg. Chem.* **2007**, 46 (10), 4187–4196.
- (76) Collison, D.; Mabbs, F. E.; McInnes, E. J. L.; Taylor, K. J.; Welch, A. J.; Yellowlees, L. J. Electrochemical and spectroelectrochemical studies on platinum complexes containing 2,2'-bipyridine. *J. Chem. Soc., Dalton Trans.* **1996**, No. 3, 329–334.
- (77) Geary, E. A. M.; McCall, K. L.; Turner, A.; Murray, P. R.; McInnes, E. J. L.; Jack, L. A.; Yellowlees, L. J.; Robertson, N. Spectroscopic, electrochemical and computational study of Pt—

- diimine-dithiolene complexes: rationalising the properties of solar cell dyes. *Dalton Trans.* **2008**, No. 28, 3701–3708.
- (78) Ray, K.; Weyhermüller, T.; Neese, F.; Wieghardt, K. Electronic Structure of Square Planar Bis(benzene-1,2-dithiolato)metal Complexes [M(L)2]z (z = 2-, 1-, 0; M = Ni, Pd, Pt, Cu, Au): An Experimental, Density Functional, and Correlated ab Initio Study. *Inorg. Chem.* **2005**, *44* (15), 5345–5360.
- (79) Ros, P.; Van Der Avoird, A.; Schuit, G. C. A. Molecular orbital calculations on copper chloride complexes. *Coord. Chem. Rev.* **1967**, 2 (1), 65–75.
- (80) Yamaguchi, K.; Takahara, Y.; Fueno, T. Ab-Initio Molecular Orbital Studies of Structure and Reactivity of Transition Metal-OXO Compounds. In *Applied Quantum Chemistry*; Smith, V. H., Schaefer, H. F., Morokuma, K., Eds.; Springer Netherlands: Dordrecht, 1986; pp 155–184, DOI: 10.1007/978-94-009-4746-7 11.
- (81) Soda, T.; Kitagawa, Y.; Onishi, T.; Takano, Y.; Shigeta, Y.; Nagao, H.; Yoshioka, Y.; Yamaguchi, K. Ab initio computations of effective exchange integrals for H–H, H–He–H and Mn2O2 complex: comparison of broken-symmetry approaches. *Chem. Phys. Lett.* **2000**, *319* (3), 223–230.
- (82) Liebscher, J.; Hartmann, H. N-Thioaroylarylthiocarboxylic acid amides and their disulfides. DD 135722A1, 1979.
- (83) Singh, B. N. Synthesis of some new 3-(arylimino)-5-p-tolyl-1,2,4-dithiazoles. *Acta Cienc. Indica, Chem.* 1998, 24 (3), 111–115.
- (84) Kuliev, A. B.; Aliev, F. Y.; Akhadov, N. O.; Rustamov, S. A. Derivatives of N-(2-pyridyl)thioamides as additives for lubricating oils. *Neftekhimiya* **1993**, 33 (4), 359–64.
- (85) Argyropoulos, N. G. Product class 2: 1,2,4-dioxazoles, 1,2,4-oxathiazoles, and 1,2,4-dithiazoles. *Sci. Synth.* **2004**, 13, 29–71.
- (86) Takajo, T.; Kambe, S.; Ando, W. Synthesis of 2,4,6-triaryl-1,3,5-dithiazines and N-arylmethylene-1-thioacylamino-1-arylmethylamines from N,N'-diarylmethylenearylmethanediamines and thioamides. *Synthesis* 1985, 1985 (1), 92–95.
- (87) Martin, R. L.; Bond, A. M.; Heath, G. A. Polarography of the planar dithioacetylacetone complexes of cobalt(II), nickel(II), palladium(II), and platinum(II) and other related complexes of the same ligand in acetone. *Inorg. Chem.* **1971**, *10* (9), 2026–32.
- (88) Murai, T.; Aso, H.; Tatematsu, Y.; Itoh, Y.; Niwa, H.; Kato, S. Reaction and Characterization of Thioamide Dianions Derived from N-Benzyl Thioamides. *J. Org. Chem.* **2003**, *68* (22), 8514–8519.
- (89) Schrauzer, G. N. Coordination compounds with delocalized ground states. Transition metal derivatives of dithiodiketones and ethylene-1,2-dithiolates (metal dithienes). *Acc. Chem. Res.* **1969**, 2 (3), 72–80.
- (90) Cowley, R. E.; Bill, E.; Neese, F.; Brennessel, W. W.; Holland, P. L. Iron(II) Complexes with Redox-Active Tetrazene (RNNNNR) Ligands. *Inorg. Chem.* **2009**, *48* (11), 4828–4836.
- (91) Suzuki, A.; Mutoh, Y.; Tsuchida, N.; Fung, C.-W.; Kikkawa, S.; Azumaya, I.; Saito, S. Synthesis and Systematic Structural Analysis of Cationic Half-Sandwich Ruthenium Chalcogenocarbonyl Complexes. *Chem. Eur. J.* **2020**, 26 (17), 3795–3802.